

Ultralow Wear Self-Mated PTFE Composites

Kylie E. Van Meter, Christopher P. Junk, Kasey L. Campbell, Tomas F. Babuska, and Brandon A. Krick*

Cite This: *Macromolecules* 2022, 55, 3924–3935

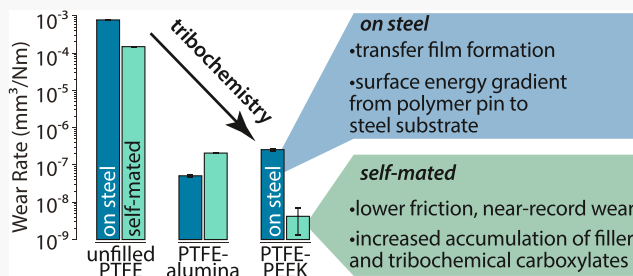
Read Online

ACCESS |

Metrics & More

Article Recommendations

ABSTRACT: Remarkably low wear rates were observed in PTFE–PEEK and polytetrafluoroethylene (PTFE)-alpha-alumina composites when evaluated in a “self-mated” configuration, where a polymer pin is slid against a polymer countersample of the same composition. Each composite was tested in a controlled humidity environment on a linearly reciprocating tribometer on two different countersamples: a polymer countersample (self-mated) and a stainless steel countersample for comparison. For all the self-mated PTFE–PEEK composites [polyether ether ketone (PEEK) wt % 10, 20, 30, 40, and 50], the average friction coefficient was reduced, and the steady-state and total specific wear rates were improved when compared to testing against stainless steel. Self-mated PTFE–PEEK (wt % 10–40) achieved ultralow wear rates on the order of 10^{-9} mm³/Nm and friction coefficients of 0.08–0.14. When compared with samples slid against stainless steel, IR spectroscopy of the sliding surface showed that the self-mated PTFE–PEEK composites accumulate more PEEK at the sliding interface and more expression of a tribochemical carboxylate species, which have been linked with ultralow wear PTFE materials. The PTFE composites slid on steel rely on the formation of transfer films for ultralow wear performance. This is achieved by unidirectional increasing surface energy gradients from the polymer pin to the steel substrate, which dominate the transport and wear of PTFE composites slid on steel. However, the self-mated ultralow wear PTFE-based composites rely only on the formation and stability of tribofilms that consist of tribochemically altered PTFE with new carboxylate end groups as well as accumulated filler (i.e., PEEK or alumina). These films have self-regulating, minimal differences in surface energy. The close match of these low-energy surfaces contributes to low friction and ultralow wear. The self-mated PEEK-filled PTFE outperforms the alumina-filled PTFE primarily because of the ease at which PEEK accumulates at the surface. Additionally, the reinforcement and anchoring of the surface is better for a polymer blend than a particle-reinforced composite.



1. INTRODUCTION

Polytetrafluoroethylene (PTFE) is widely used in tribological applications due to its low friction, high melting temperature and operating range, and hydrophobic properties.^{1–5} However, PTFE is prone to high wear rates ($K \sim 10^{-4}$ mm³/Nm).^{6–11} Filler materials can be added to PTFE to improve its wear characteristics by 3–5 orders of magnitude. By adding less than 5 wt % of microscale alpha-alumina particles, the wear rate of the composite can be reduced to 10^{-7} mm³/Nm or less.^{11–18} PTFE can also be blended with other polymeric materials, such as polyether ether ketone (PEEK), to improve wear rates by several orders of magnitude.^{19–21} The fillers appear to serve multiple functions for wear reduction, including preventing delamination,^{10,12,19,22,23} reducing debris size,^{24–26} and stabilizing the characteristic transfer films^{12,13,21,27–29} and running films.¹⁶

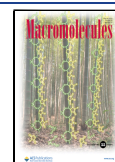
While the specific mechanisms behind the role of fillers in transfer film development vary between filler materials and are not fully understood, the transfer films of ultralow wear PTFE composites ($K < 10^{-7}$ mm³/Nm) usually exhibit chemical changes generated through a combination of the physical sliding motion and environmental factors.^{17,18,20,21,26,30,31} In

works by Harris et al., critical contact lengths of PTFE fibrils to fracture due to sliding were computed and concluded that high molecular weight PTFE fibrils are unlikely to transfer an entire polymer chain to the surface and C–C backbone bond scission occurs during sliding.¹³ Fluoropolymers with lower molecular weights will have higher crystallinity, which was observed by Sidebottom et al. using differential scanning calorimetry analysis of perfluoroalkoxy polymer wear debris compared to the bulk material, indicating that sliding induces chain scission and chain shortening.³² Shear-induced polymer chain scission of PTFE C–C bonds and reactions with the sliding countersample and environment can generate carboxylic acid end groups which are observable through IR spectroscopy.^{16,18,20,21} These chemical species are only present after sliding, indicating that there are chemical differences between

Received: December 17, 2021

Revised: April 27, 2022

Published: May 12, 2022



the bulk polymer and the tribofilms (i.e., polymer transfer film on the countersample and running film on the wear surface of the polymer). Running films have also been shown to have higher hardness and elastic moduli than the bulk polymer.¹⁶ These tribochemical changes and more robust mechanical properties of tribofilms contribute to the improved wear properties in PTFE composites.^{12,16,18,20–22,32–35}

The low-friction sliding of PTFE and PTFE composites is attributed to the easy relative shearing of units of PTFE and PTFE sliding on the transfer film formed on the opposing material at the sliding interface. PTFE structural units, or crystallites, contain slices of closely packed and folded polymer chains. These slices are separated by amorphous or poorly crystalline regions; during sliding, PTFE adheres to the sliding countersurface, and the amorphous polymer regions are sheared with relatively low stresses.³⁶ In many tribological experiments and applications, PTFE composites slide against steel alloys. The steel countersurface is much harder than the PTFE composite and shears the softer PTFE during sliding. The sheared material is deposited onto the steel countersurface, forming a thin transfer film. In situ surface plasmon resonance experiments have shown that PTFE will transfer to the sliding countersurface in as low as 1 sliding cycle.³⁷ Due to PTFE's low surface energy and rigid, fluorine-encased polymer chain structure, the bulk composite of PTFE can slide against the thin transfer film with low forces and very low friction coefficients ($\mu < 0.1$).⁶ Ultimately, both the low friction and low wear properties of PTFE composites can be mainly attributed to well-developed transfer films that are persistent throughout sliding.

The observation of low friction and low wear of PTFE composites in sliding experiments where robust transfer films can be formed points to the importance of PTFE composites sliding against a deposited layer of the PTFE composite itself. The characteristic tribochemical changes seen in ultralow wear PTFE composite transfer films are important for the physical bonding of the transfer film to the countersample and the subsequent reduction in film delamination. Based on this, it is possible that the sliding of a PTFE composite against a countersurface made of the same PTFE composite could result in low friction and wear. In this paper, the wear and friction behavior of PTFE composites slid against compositionally identical PTFE composites in a "self-mated" configuration were investigated. Various PTFE composites (unfilled PTFE, PTFE-PEEK, and PTFE-alpha-alumina) were tested in both a self-mated configuration (composite on composite) and a control (composite on stainless steel). Wear rate and friction coefficient were measured to observe the differences in performance and potentially lower friction and lower wear behavior in a self-mated configuration. IR spectroscopy of the bulk polymer and the polymer wear surface (often referred to as a "running film") was used to evaluate if tribochemical changes also occur in self-mated sliding when compared to composite-on-steel sliding.

2. MATERIALS AND METHODS

2.1. Materials and Sample Preparation. Seven different PTFE-filled composites were evaluated: PTFE (Chemours Teflon 7C resin) with 10, 20, 30, 40, and 50 wt % PEEK (450PF, Victrex), unfilled PTFE, and PTFE with 5 wt % alpha-alumina (Nanostructured and Amorphous Materials, Inc., Stock #1015WW,99.5%). The alumina has a supplier-specified approximate particle size of 27–43 nm (no method given); however, it has been shown that the filler has a

median size of $\sim 4 \mu\text{m}$ as measured by static light scattering. Furthermore, the filler has a porous/agglomerated architecture with nanoscale features.¹²

The dry powders were combined and mixed by hand using a spatula, after which isopropyl alcohol (IPA) was added (at a ratio of $\sim 5:1$ alcohol to powder by mass) and mixed. The samples were further combined using an ultrasonic horn (Branson Digital Sonifier SFX550) with a micro-tip attachment. Sonication was performed at 40% amplitude for three continuously pulsed 5 min intervals, with a rest in between intervals of 1 min or until the mixtures were allowed to cool down to room temperature. The IPA-dispersed samples were placed in a fume hood to allow the IPA to fully evaporate over the course of 3–5 days.

The mixed composite resin powder (50 g) was placed in a rectangular $1" \times 2.5"$ ($25.4 \text{ mm} \times 63.5 \text{ mm}$) 440 C stainless steel mold and compressed to 10 MPa using a hydraulic press. The molded sample was wrapped in aluminum foil and free-sintered in an oven using the following temperature profile: heated at $2^\circ\text{C}/\text{min}$ from room temperature to 380°C , 3 h dwell at 380°C , and cooled at $2^\circ\text{C}/\text{min}$ from 380°C to room temperature. The sintered sample was used to make both the pin and the countersample. An $8 \text{ mm} \times 25 \text{ mm}$ section of the molded sample was cut off and machined to make two $6.35 \times 6.35 \times 12 \text{ mm}$ pins. The remaining material was used as the countersample for self-mated testing. Four holes were drilled to serve as attachment points.

In addition to the self-mated testing, one of the two machined polymer pins was also tested on a 304 stainless steel countersample for comparison with the self-mated results and with previously reported wear performance. A $0.1875" \times 1" \times 1.5"$ mirror finish 304 stainless steel coupon was used for testing. The real surface roughness was measured to be 25 nm Ra using an optical profilometer.

Prior to testing, polymer pins and countersamples were submerged in methanol and sonicated for 30 min. The samples were removed and placed in a fume hood to dry. Stainless steel countersamples were washed with Alconox soap, rinsed with water, and then rinsed with methanol. The countersamples were also placed in a fume hood to dry. After drying, the polymer samples were allowed to equilibrate in the controlled humidity chamber used for testing.

2.2. Friction and Wear Testing. Friction and wear testing was performed in a flat-on-flat sample configuration (Figure 1) on a linear

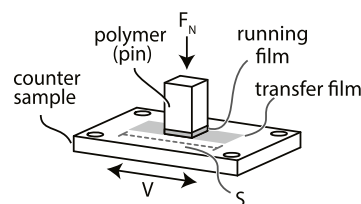


Figure 1. Flat-on-flat configuration of polymer pin and the countersample.

reciprocating tribometer. A 250 N normal force was applied, resulting in a contact pressure of 6.2 MPa. Two load cells continuously measured the normal and friction forces experienced by the polymer pin. A constant contact pressure was maintained by servoing on the measured normal load. The countersample was slid below the polymer pin over a stroke length of 20 mm (40 mm/cycle) and a speed of 50 mm/s using a larger ball screw-driven stage. The samples were slid for a total of 1 million cycles (40 km of sliding). Interrupted mass measurements were performed at the following cycle intervals: 1k, 4k, 5k, 10k, 10k, 10k, 10k, 50k, 100k, 100k, 100k, 100k, 200k, and 200k. All experiments were performed in an environmentally controlled glovebox with air at a $30 \pm 2\%$ RH with an ambient temperature of $24\text{--}26^\circ\text{C}$. The sample temperature was not directly measured. While we did not test multiple normal loads, we present specific wear rates as they are the most broadly applicable across the literature. Sliding speeds, contact pressures, and contact geometries used in testing are comparable to many previous works on

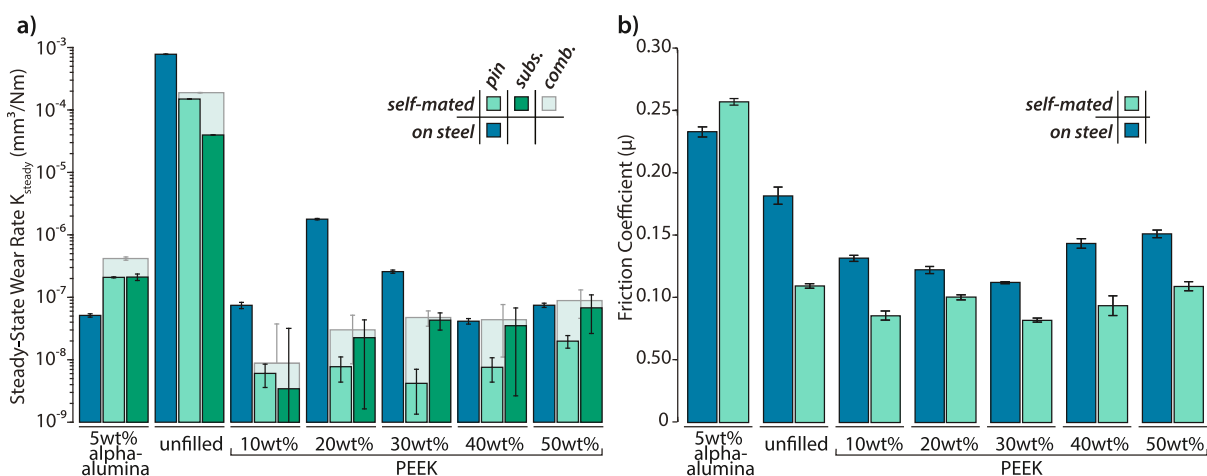


Figure 2. (a) Steady-state wear rates of PTFE composites slid against stainless steel countersamples and self-mated polymer countersamples. Wear reported for polymer pins slid on steel, polymer pin slid self-mated against a polymer countersample, and the wear of the polymer countersample itself. (b) Friction coefficients of PTFE composites slid against stainless steel countersamples and self-mated polymer countersamples. The friction coefficient reported is the average friction coefficient measured during sliding over the steady-state wear region.

Table 1. Summary of Tribological Results

filler	countersample	μ_{steady}	σ_{μ}	K_{steady} (mm^3/Nm)	$U_{K_{\text{steady}}}$ (mm^3/Nm)	K_{total} (mm^3/Nm)	$U_{K_{\text{total}}}$ (mm^3/Nm)
5 wt % Al_2O_3	steel (pin)	0.234	0.004	5.1×10^{-8}	3.3×10^{-9}	1.4×10^{-7}	1.2×10^{-9}
	self (pin)	0.258	0.003	2.1×10^{-7}	3.8×10^{-9}	2.0×10^{-7}	1.5×10^{-9}
	self (sub.)	0.258	0.003	2.1×10^{-7}	2.5×10^{-8}	1.9×10^{-7}	9.3×10^{-9}
10 wt % PEEK	steel (pin)	0.132	0.002	7.5×10^{-8}	8.6×10^{-9}	5.1×10^{-7}	2.6×10^{-9}
	self (pin)	0.086	0.004	4.8×10^{-9}	3.2×10^{-9}	5.8×10^{-8}	1.3×10^{-9}
	self (sub.)	0.086	0.004	3.2×10^{-9}	2.7×10^{-8}	4.3×10^{-7}	1.1×10^{-8}
20 wt % PEEK	steel (pin)	0.123	0.003	1.8×10^{-6}	4.6×10^{-8}	3.0×10^{-6}	1.5×10^{-8}
	self (pin)	0.101	0.002	7.9×10^{-9}	3.5×10^{-9}	1.3×10^{-7}	1.2×10^{-9}
	self (sub.)	0.101	0.002	2.2×10^{-8}	2.1×10^{-8}	4.9×10^{-7}	7.9×10^{-9}
30 wt % PEEK	steel (pin)	0.113	0.001	2.6×10^{-7}	1.5×10^{-8}	9.7×10^{-7}	4.5×10^{-9}
	self (pin)	0.082	0.002	4.1×10^{-9}	2.8×10^{-9}	4.4×10^{-8}	1.1×10^{-9}
	self (sub.)	0.082	0.002	4.3×10^{-8}	1.3×10^{-8}	2.5×10^{-7}	5.1×10^{-9}
40 wt % PEEK	steel (pin)	0.144	0.004	4.2×10^{-8}	4.2×10^{-9}	1.9×10^{-7}	1.4×10^{-9}
	self (pin)	0.094	0.008	7.5×10^{-9}	3.3×10^{-9}	1.1×10^{-7}	1.2×10^{-9}
	self (sub.)	0.094	0.008	3.6×10^{-8}	3.2×10^{-8}	2.5×10^{-7}	1.3×10^{-8}
50 wt % PEEK	steel (pin)	0.152	0.003	7.5×10^{-8}	6.0×10^{-9}	3.4×10^{-7}	1.9×10^{-9}
	self (pin)	0.110	0.004	2.0×10^{-8}	4.4×10^{-9}	2.2×10^{-7}	1.5×10^{-9}
	self (sub.)	0.110	0.004	7.1×10^{-8}	4.3×10^{-8}	7.2×10^{-7}	1.7×10^{-8}
unfilled	steel (pin)	0.182	0.007	7.8×10^{-4}	5.6×10^{-6}	7.8×10^{-4}	3.6×10^{-6}
	self (pin)	0.110	0.002	1.5×10^{-4}	1.1×10^{-6}	1.3×10^{-4}	5.9×10^{-7}
	self (sub.)	0.110	0.002	4.0×10^{-5}	2.7×10^{-7}	3.1×10^{-5}	1.5×10^{-7}

PTFE composites, and based on the studies on the tribological properties of PTFE and PTFE–PEEK composites, should not cause any significant frictional heating or creep of the sample.^{6,10,12,19–21,25}

Prior to testing, the polymer pins and polymer countersamples were massed on a scale (Mettler Toledo XS205DU, 0.00001 g resolution), and the dimensions of the samples were measured using calipers (Mitutoyo AOS, 0.01 mm resolution). Material density was determined using the volume of the sample and its mass (for polymer countersamples, the volumes of the drilled attachment holes were accounted for in density calculations). Interrupted mass measurements were performed during the cycle intervals mentioned previously. Volume loss was determined using the mass loss of the sample and the material density. The specific wear rate of the sample K was calculated using eq 1, where V is the volume loss of the sample, F_N is the applied load, and d is the sliding distance.

$$K[\text{mm}^3/\text{Nm}] = \frac{V[\text{mm}^3]}{F_N[\text{N}]d[\text{m}]} \quad (1)$$

Several types of specific wear rates were examined. Total wear rate K_{tot} can be calculated using the total volume loss of the sample and the total sliding distance. Incremental wear rates K_{inc} are calculated using the volume loss per cycle interval and the sliding distance during that interval. Steady-state wear rates K_{ss} and associated uncertainties were calculated using a three-point fit using methods described in ref 38. The steady-state wear rates were calculated in regions of the sliding distance where the volume loss exhibits a linearly increasing trend.

Friction coefficients and their standard deviations were calculated using the methods described in ref 39. The measured friction force was divided by the measured normal force and plotted over the linear sliding position for each cycle, creating a friction loop. The middle 50% of the loop was averaged to determine the friction coefficient for each sliding cycle (as in ref 39).

2.3. Infrared Spectroscopy. A PerkinElmer Spectrum 100 Fourier transform infrared (FT-IR) spectrometer with an attenuated total reflectance (ATR) accessory was used to identify the chemical changes that occurred at the sliding interface of tribologically tested

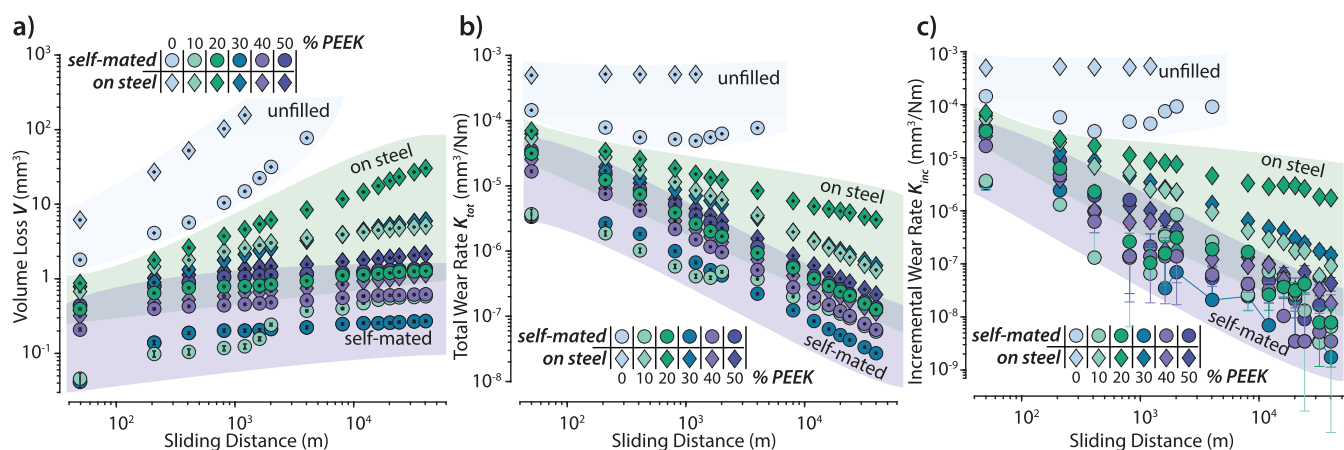


Figure 3. (a) Volume loss of PTFE composites over the total sliding distance. (b) Total wear rate of PTFE composites over the total sliding distance. (c) Incremental wear rate over the total sliding distance. Note: Log scales for all axes.

PTFE composites. Both the sliding surface (tested surface) and the bulk polymer (untested surface) for all composites were examined. All spectra collected consisted of 32 scans with a spectral resolution of 4 cm^{-1} . The spectra were collected by cleaning the ATR diamond crystal with isopropanol alcohol, followed by a background scan. ATR measurements were made by placing the entire polymer sample wear surface in contact with the diamond crystal and applying a normal force using a manual probe, resulting in a spectra that samples the entire surface. Baseline subtraction was performed using the PerkinElmer Spectrum software's baseline subtraction feature.

3. RESULTS AND DISCUSSION

3.1. Wear and Friction of Self-Mated PTFE Composites. The PTFE–PEEK composites as well as the unfilled PTFE showed lower wear rates and lower friction coefficients in the self-mated configuration as compared to those slid on steel (Figure 2 and Table 1). However, in the case of PTFE with 5 wt % alumina, the friction coefficient and wear rate were both moderately higher in the self-mated configuration than when slid against stainless steel (Figure 2, Table 1).

The self-mated 30 wt % PEEK pin had the lowest steady-state wear rate of all samples tested ($4.14 \times 10^{-9} \text{ mm}^3/\text{Nm}$) as well as the lowest friction coefficient of 0.082. The unfilled PTFE on steel had the highest steady-state wear rate of all samples tested ($7.80 \times 10^{-4} \text{ mm}^3/\text{Nm}$), but the self-mated 5 wt % alpha-alumina pin had the highest steady-state friction coefficient of 0.258.

The average steady-state friction coefficient (μ_{steady}), steady-state wear rate (K_{steady}), and total wear rate (K_{total}) with associated standard deviation (σ_{μ}) and uncertainties ($U_{K_{\text{steady}}}$ and $U_{K_{\text{total}}}$) measured for all PTFE composites tested are presented in Table 1. The values are reported for the polymer pin slid against steel (steel (pin)), the self-mated pin (self (pin)), and the self-mated polymer countersample (self (sub.)).

3.2. PTFE/PEEK Composites. A weight percent series of PTFE–PEEK samples (10, 20, 30, 40, and 50 wt %) was tested on steel and on a self-mated polymer countersample. All self-mated samples exhibited lower friction and wear behavior when compared to the same material slid against a stainless steel countersurface. All self-mated pin samples except 50 wt % PEEK achieved ultralow wear rates on the order of $10^{-9} \text{ mm}^3/\text{Nm}$ (Figure 2a). All self-mated samples including the 50 wt % samples had friction coefficients lower than 0.11 and as low as 0.08 (Figure 2b). However, not all samples slid against steel

performed in a similar manner. The wear performance of the samples slid on stainless steel varied from orders 10^{-6} to $10^{-8} \text{ mm}^3/\text{Nm}$, with no correlation to the wear rates of the self-mated samples. The friction coefficients when slid against steel ranged from 0.12 to 0.15.

The steady-state wear rates of almost all the self-mated pins reached below $2 \times 10^{-8} \text{ mm}^3/\text{Nm}$ (as low as $4.1 \times 10^{-9} \text{ mm}^3/\text{Nm}$); however, the wear rates of the self-mated countersamples were generally higher than the self-mated pins, between 2 and $7 \times 10^{-8} \text{ mm}^3/\text{Nm}$ but with the 10 wt % reaching as low as $3 \times 10^{-9} \text{ mm}^3/\text{Nm}$ (Table 1).

There were no observable trends in wear rate or friction coefficient related to wt % of filler for either self-mated or on steel configurations. However, all self-mated pins from the 10–40 wt % range achieved $10^{-9} \text{ mm}^3/\text{Nm}$ steady-state wear rates (50 wt % $\sim 2 \times 10^{-8} \text{ mm}^3/\text{Nm}$), and all countersamples achieved $10^{-8} \text{ mm}^3/\text{Nm}$ steady-state wear rates, regardless of PEEK filler percentage. The wear rates of the pins on steel varied multiple orders of magnitude depending on filler percentage (10^{-6} to $10^{-8} \text{ mm}^3/\text{Nm}$). This indicates that the inherent variability in wear performance often seen in PTFE–PEEK (e.g., Burris and Sawyer reported PTFE–PEEK composite wear rates can vary by 2 orders of magnitude at comparable filler weight percentages in batch variations¹⁹) can be mitigated by running these materials in a self-mated configuration.

Trends in wear performance can be more closely investigated in Figure 3 where volume loss, total wear rate, and incremental wear rate are plotted over sliding distance. In Figure 3a, the wear volume of all self-mated PTFE–PEEK pins are bounded below $\sim 1 \text{ mm}^3$, regardless of filler wt %. There is a small amount of overlap between the upper bound of the self-mated samples and the lower bound of the samples slid against steel. This overlap in volume loss and total wear rate between self-mated and on-steel is due to the markedly low wear of the PTFE 40 wt % PEEK slid against steel as compared to the other samples slid on steel, the lowest of any sample slid against steel in the entire data set.

The total wear rate trends of the PTFE–PEEK samples were very similar to the volume loss trends, shown in Figure 3b. A small amount of overlap between the self-mated and the on-steel total wear bounds can also be attributed to the relatively high wear of the self-mated 50 wt % PEEK sample and the relatively low wear of the 40 wt % PEEK sample slid against

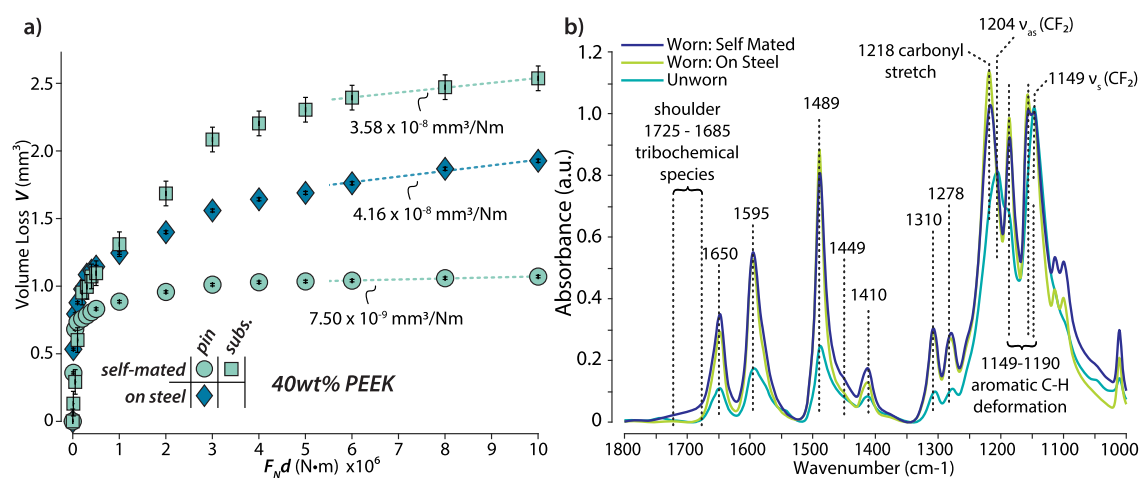


Figure 4. (a) Volume loss of PTFE 40 wt % PEEK run against steel and self-mated countersample plotted over $F_N d$. Specific steady-state wear rate is indicated by the dashed line plotted for each sample. (b) ATR-IR spectra of the worn surface of PTFE 40 wt % PEEK run against steel, the worn surface run self-mated, and the bulk unworn composite.

Table 2. Peak Assignments of IR Spectra of Worn PTFE/Alumina and PTFE/PEEK Composites

peak location (cm ⁻¹)	source	IR assignment	found in:	citation
1685–1725	Tribochemical	R_F -carboxylate salts (monodentate and bridging)	PTFE–PEEK and PTFE-alumina	13,18,20,21,40,41
1660	tribochemical	R_F -carboxylate	PTFE–PEEK and PTFE-alumina	13,18,20,21,40,41
1650	PEEK	PEEK marker	PTFE–PEEK	20,21
1595	PEEK	PEEK marker	PTFE–PEEK	20,21
1489	PEEK	PEEK marker	PTFE–PEEK	20,21
1449	tribochemical	chelated R_F -carboxylic acid	PTFE–PEEK	13,18,20,21,40,41
1430	tribochemical	chelated R_F -carboxylic acid	PTFE-alumina	13,18,20,21,40,41
1410	PEEK	PEEK marker	PTFE–PEEK	21,42
1360	PTFE	shortened PTFE chains	PTFE-alumina	33,43,44
1310, 1315	PTFE	shortened PTFE chains	PTFE–PEEK, PTFE–alumina	33,43,44
1278	PTFE	chain alignment	PTFE–PEEK	13,18,33,45
1218	PEEK	carbonyl stretch	PTFE–PEEK	20,21
1204	PTFE	asymmetric stretching of CF ₂	PTFE–PEEK and PTFE-alumina	13,18,20,21,33,46
1149–1190	PEEK	aromatic C–H deformation	PTFE–PEEK	21
1149	PTFE	symmetric stretching of CF ₂	PTFE–PEEK and PTFE-alumina	13,18,20,21,33,46
800	Alumina	aluminum oxide	PTFE-alumina	32

steel. In Figure 3c, incremental wear rates had a similar overlap, especially in the larger sliding distances. This figure also demonstrates the distance of sliding required for samples to achieve steady-state wear. For most self-mated samples, steady-state wear (constant incremental wear) was not achieved until 20 km of sliding or more. Additionally, most samples slid on steel took a comparable amount of sliding distance to also achieve steady-state wear. This transition from initially high wear rates to low steady-state wear rates is commonly referred to as “run-in”.

The 40 wt % PEEK samples had the most similarity between the steady-state wear self-mated and on-steel and also had the lowest wear rate on steel of any of the samples. The steady-state wear rates were plotted on the (volume loss) versus (normal load times distance) plot shown in Figure 4a (Note: the slope of this plot is the wear rate in mm³/Nm). The run-in volume of the self-mated pin is several times lower than both the pin on steel and self-mated countersamples. However, the volume loss of the pin on steel is lower than the pin on the self-mated countersample despite the steady-state wear rate of the self-mated countersample being less than the pin on steel. When considering the combined volume loss and wear rate of the self-mated pairing, the combined volume loss is higher than

the pin-on-steel, but the steady-state wear is the same as the pin on steel (4.4 and 4.2×10^{-8} mm³/Nm, respectively). It is also important to note that the uncertainty in the steady-state wear of the self-mated countersample is 3.2×10^{-8} mm³/Nm, which is on the order of the steady-state wear itself. This can be attributed to the volume loss fluctuations as the countersample approaches steady state as well as the very low volume loss relative to the overall volume of the sample. This high uncertainty indicates that further sliding cycles are needed to improve the uncertainty of the measurement and potentially reveal even lower steady-state wear rates as the countersample continues to run in.

To understand the tribochemical differences between the running films of each sample, IR spectra were collected for the worn surfaces of the self-mated and on-steel samples as well as the bulk unworn composite for comparison. The absorbance spectra of each 40 wt % sample are plotted in Figure 4b. All spectra were normalized to the 1149 cm⁻¹ peak. The spectral identification of new tribochemical species in the region between 1400 and 1700 cm⁻¹ was challenging in this polymer/polymer composite due to the multiple large absorbances of the PEEK backbone (carbonyls and aromatic ring-breathing modes) overlapping with those of new perfluorinated

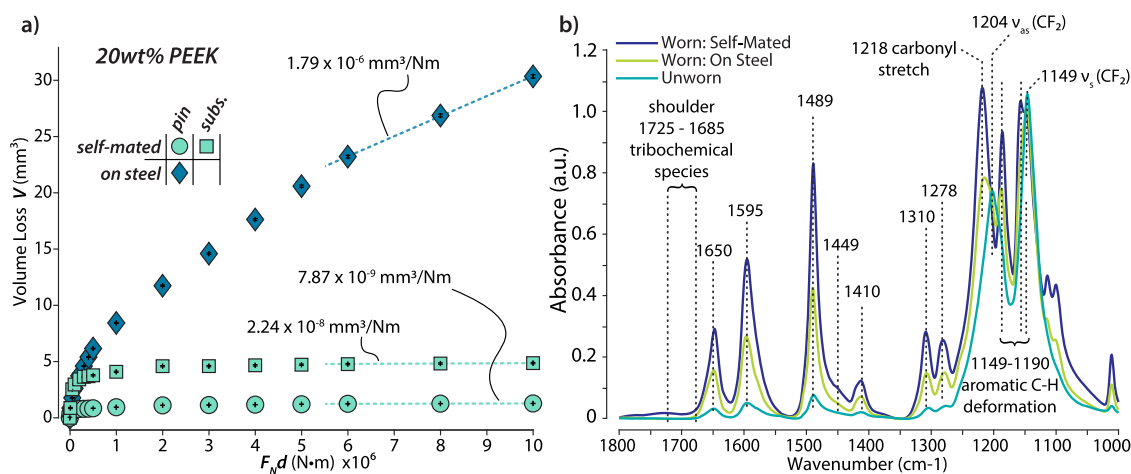


Figure 5. (a) Volume loss of PTFE 20 wt % PEEK run against steel and self-mated countersample plotted over $F_N d$. The specific steady-state wear rate is indicated by the dashed line plotted for each sample. (b) IR spectra of worn surface of PTFE 20 wt % PEEK run against steel, the worn surface run self-mated, and the bulk unworn composite. All absorbance data was normalized to the 1149 cm^{-1} PTFE CF_2 peak.

carboxylic acid end groups.^{20,21} Peaks at 1149 and 1204 cm^{-1} , characteristic of PTFE, correspond to symmetric and asymmetric stretching of CF_2 units in the backbone (Table 2). Peaks in the $1149\text{--}1190\text{ cm}^{-1}$ range are aromatic C–H deformations, characteristic of PEEK. Peaks at 1650 , 1595 , 1489 , and 1410 cm^{-1} are also markers for PEEK. The peak at 1218 cm^{-1} corresponds to a carbonyl stretch, also associated with PEEK. Both the self-mated and on-steel samples showed differences in absorbance spectra when compared to the bulk unworn composite. The change in ratio of infrared peaks for the two polymers denotes an accumulation of PEEK at the sliding interface. The shoulders present in the $1725\text{--}1685\text{ cm}^{-1}$ range and at 1449 cm^{-1} are characteristic of perfluorinated carboxylate salt formation, which were not present in the unworn sample. These new peaks have been observed by multiple groups in recent years and strongly correlate with tribochemical species that only accumulate in ultralow wear samples [13], [20], [21], [32], [36], [37]. The shoulder of the self-mated sample is more pronounced than that of the on-steel sample, and the additional carboxylic salt accumulation could explain the lower steady-state wear rates of the self-mated sample.

Other samples, such as the 20 wt % PEEK, had a much larger difference in performance between the self-mated and on-steel configurations. As shown in Figure 5a, the volume loss of the pin run on steel was over an order of magnitude higher than the self-mated pin. The steady-state wear of the sample on steel was $1.79 \times 10^{-6}\text{ mm}^3/\text{Nm}$, 2 orders of magnitude higher than the self-mated countersample and 3 orders of magnitude higher than the self-mated pin. The wear rate of PTFE with 20 wt % PEEK on steel was unexpectedly high, as the PEEK loadings at or near 20% are often very low in many of the previous studies of this material.^{19–21} On looking back, the original report on this material by Burriss et al. showed a large variation in the wear rates of this material, even at comparable loading percentages.¹⁹ This suggests that there must be some unknown processing variable that causes batch-to-batch variation. However, self-mated configurations seem to be less sensitive to batch variabilities, providing a more reliable ultralow wear tribological pair.

The significant differences in the wear rate of the self-mated and on-steel PTFE-20 wt % PEEK sample also correlated with

differences in IR spectra (Figure 5b). Unlike the spectra of the 40 wt % PEEK samples, the relative peak intensities of the worn self-mated and worn on steel were quite different. The much larger absorbances at 1650 , 1595 , 1489 , and 1410 cm^{-1} denoted a higher level of PEEK accumulation at the sliding interface. In addition, the shoulder in the $1685\text{--}1725\text{ cm}^{-1}$ region was present for the self-mated pin but not for the pin on steel. The lack of this shoulder in the pin slid on steel indicates a lack of tribochemical development, which has been correlated with higher wear rates.²¹ When comparing the PEEK accumulation at the wear interface of the self-mated and on-steel samples, the self-mated samples generally have more PEEK build-up.

For all PTFE–PEEK samples tested, the transition from initially high wear rates to low steady-state wear rates of the countersamples lagged behind the run in of the pins (see Figures 4a and 5a). This could be attributed to the slower development of tribochemistry on the countersample. The stroke length during testing was 20 mm (40 mm/cycle), while the width of the pin was ~ 6.35 mm. Over the course of a sliding cycle, only 32% of the countersample track length was in contact with the pin at any given time, while the pin was in constant contact. This could cause the pin to develop a tribofilm at a faster rate than the countersample, as any given point on the pin experienced ~ 3.1 times more slip distance than a point on the countersample. At the conclusion of testing, all pins tested had achieved steady-state wear. However, it is possible that the countersamples were still in a transient period of run in. It is hypothesized that further testing (past 1 million cycles) might result in equal pin and countersample wear rates. Additionally, some interesting things might be observed by varying the stroke distance relative to the pin width.

While PTFE–PEEK composites are reported to be among the most wear-resistant polymers ever recorded,⁴⁷ repeated measurements resulted in a wide range of wear rates, pointing to an uncontrolled element of this material's remarkable performance. This was highlighted in the seminal paper by Burriss and Sawyer where mixtures of comparable ratios (nominally ~ 15 wt % PEEK as measured gravimetrically) had wear rates ranging from 5×10^{-9} to $2 \times 10^{-7}\text{ mm}^3/\text{Nm}$.¹⁹ Subsequent manuscripts were unable to achieve wear rates of

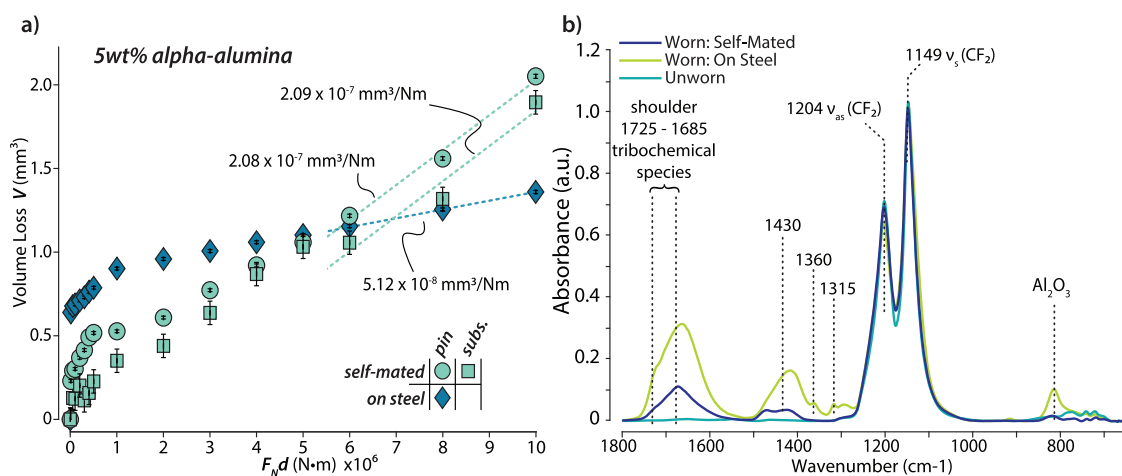


Figure 6. (a) Volume loss of PTFE 5 wt % alpha-alumina samples slid on a steel countersample and slid on a self-mated polymer countersample plotted over $F_N d$. Specific steady-state wear rate is indicated by the dashed line plotted for each sample. (b) IR spectra of worn surface of PTFE/5 wt % alpha-alumina run against steel, the worn surface run self-mated, and the bulk unworn composite. All absorbance data were normalized to the 1149 cm^{-1} PTFE CF_2 peak.

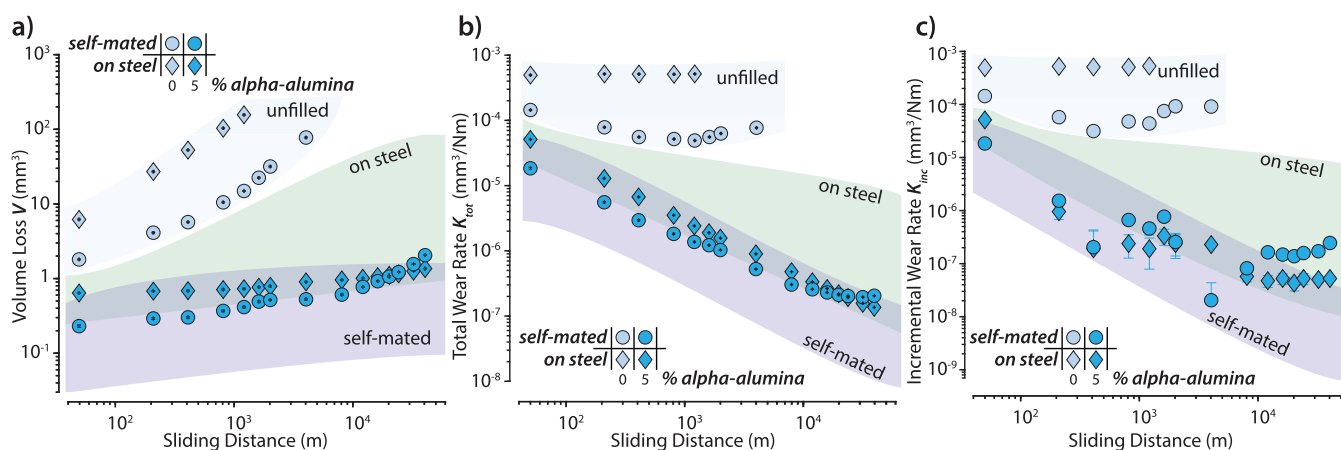


Figure 7. (a) Volume loss of alpha-alumina and unfilled PTFE composites over the total sliding distance. (b) Total wear rate of alpha-alumina and unfilled PTFE composites over the total sliding distance. (c) Incremental wear rate over the total sliding distance. Note: Log scales for all axes.

PEEK–PTFE below $1 \times 10^{-8}\text{ mm}^3/\text{Nm}$.^{20,21} Hypotheses for this behavior range from thermal processing and resulting microstructure¹⁹ to trace alumina filler contaminants.^{14,15} Regardless of the origins of this variability in wear behavior, the effects seem to be mitigated by the self-mated configuration. Furthermore, the wear rates and friction coefficients are always lower for self-mated PTFE–PEEK composites.

3.3. PTFE–Alumina Composites. PTFE-5 wt % alumina samples run on steel achieved a steady-state wear rate of $5.1 \times 10^{-8}\text{ mm}^3/\text{Nm}$. When run in a self-mated configuration, the PTFE alumina pin and polymer countersample achieved steady-state wear rates of $2.1 \times 10^{-7}\text{ mm}^3/\text{Nm}$. In Figure 6a, the volume loss of the samples was plotted over the normal force times the sliding distance. The slopes of the lines plotted indicate the steady-state specific wear rate of each sample. The volume loss of the self-mated sample started off with a smaller run-in region shown in Figure 6a and a lower total volume loss prior to 18 km of sliding when compared to the sample run on steel. The self-mated volume loss appeared to level out and started to achieve a lower wear rate [$K \sim 2 \times 10^{-8}\text{ mm}^3/\text{Nm}$ at 4 km of sliding (Figure 7c) or 10^6 Nm (Figure 6a)]. However, a wear event occurred after 4 km of sliding, and the

incremental wear rate started to increase as can be seen in Figure 7c. Beyond this point, the wear rate of the self-mated sample exceeded that of the sample on steel. The countersample achieved roughly the same steady-state wear rate as the self-mated pin ($K \sim 2.1 \times 10^{-7}\text{ mm}^3/\text{Nm}$).

IR spectra of the PTFE-5 wt % alumina running films showed much larger peaks at 1685 and 1430 cm^{-1} when slid against steel than when slid self-mated, indicating a higher development of tribochemistry. As observed by various other research groups, the peaks in these regions correspond to R_F -carboxylate salts, which have been shown to be present in the tribofilms of ultralow wear materials.^{18,20–22} These tribochemical species serve as functional groups to (1) chemically bond PTFE transfer films to the countersample, thereby anchoring the films, and (2) bond PTFE chains to the reinforcing accumulated metal oxide filler fragments and metals (worn from the countersample), effectively increasing the hardness and modulus of the tribofilms.¹⁶ The larger expression of tribochemistry coincided with the lower wear observed in the PTFE-5 wt % alumina sample run against steel. The lack of tribochemical development in the self-mated sample indicated a potentially less robust tribofilm forming at the sliding interface. This could explain the large wear event which

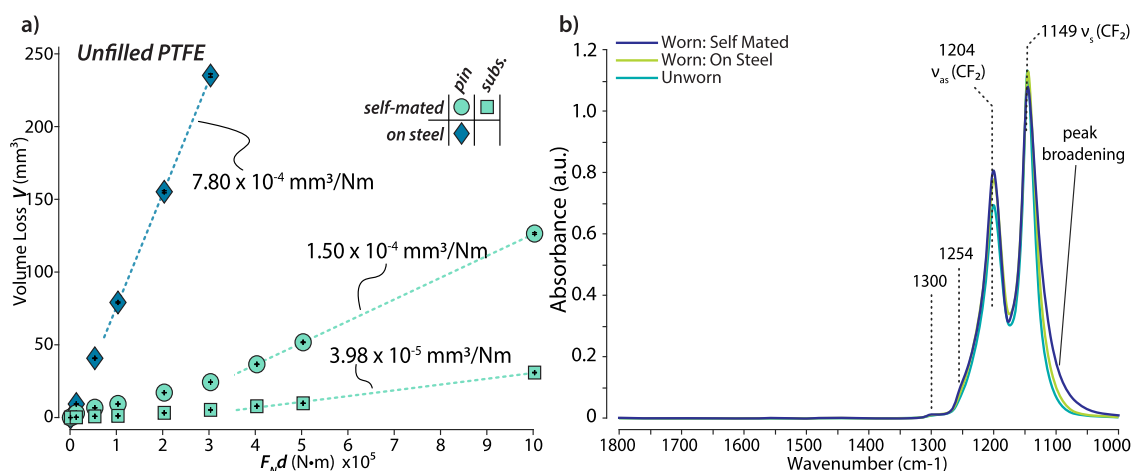


Figure 8. (a) Volume loss of unfilled PTFE samples slid on a steel countersample and slid on a self-mated polymer countersample plotted over $F_N d$. Specific steady-state wear rate is indicated by the dashed line plotted for each sample. (b) IR spectra of worn surface of unfilled PTFE run against steel, the worn surface run self-mated, and the bulk unworn polymer.

occurred at 4 km of sliding and the subsequent higher steady-state wear when compared to the sample on steel. Prior to the large wear event, the incremental wear rate of the self-mated PTFE-5 wt % alumina sample was lower than the sample run on steel. The lower IR absorbance in these regions could also be attributed to a delaminated running film, where after the large wear event at 4 km, some of the running film was removed such that there was simply less tribochemical species left on the surface.

Peaks at 1315 and 1360 cm^{-1} can be attributed to axial stretching of CF_2 and the presence of relatively short PTFE polymer chains^{33,43,48} (Table 2). In previous work, these peaks were only observed when the fluorocarbon chains were short.⁴³ Decreasing chain length can be caused by sliding-induced chain scission. Peaks 1315 and 1360 cm^{-1} in the running film of the PTFE/5 wt % alumina slid against steel indicated the presence and accumulation of these short fluorocarbon chains. The chain scission of PTFE is critical to the formation of tribochemistry and tribofilms.^{13,22} The lack of these peaks in the self-mated sample indicates either a lack of accumulation of these short PTFE chains in the transfer film or the self-mated system does not generate shortened PTFE chains. This contrast between the self-mated and on-steel configuration supports the differences seen in their tribochemical expression and wear performance.

Wear and tribofilm formation mechanisms for PTFE filled with alumina microfillers have been widely studied.^{11,13,15–18,22,31,49} It has been demonstrated that the accumulation of alumina in the transfer film and the running film helps to reduce wear by reinforcing the composite.^{16,18,21,33} In those systems, it was necessary that the alumina microfillers be friable enough to be broken down into nanoscale fragments, which then accumulated at the sliding interface and bonded to newly formed carboxyl end groups.^{12,21} If the particulates were hard or remained at the microscale, they abraded the transfer film and/or countersurface which led to delamination and large wear events.

It is possible that, when sliding in a self-mated configuration, the degree to which these microscale fillers encounter a hard-enough body or reach a high-enough stress to break down into nanoscale fragments is limited. Even if they did contact another particle, the frequency of these contacts would be

significantly less than the frequency of which they interact with steel. Thus, it is less likely to form the inherently wear-resistant alumina-rich tribofilms previously observed with PTFE-alumina on steel.^{13,18,32} If the alpha-alumina remained in its microscale state, it could become a source of abrasion and wear of developed tribofilms.

3.4. Unfilled PTFE. The unfilled PTFE sample exhibited steady-state wear and friction that was lower in the self-mated configuration than the sample run on stainless steel. Figure 7a shows that the volume loss of the unfilled PTFE slid on stainless steel is linear from the beginning of testing. This linearity can be observed in Figure 7b,c, where the incremental wear is constant, and the total wear is constant. The steady-state wear was determined to be $7.4 \times 10^{-4} \text{ mm}^3/\text{Nm}$. The self-mated unfilled PTFE sample was observed to be much more variable over the course of testing. Prior to 800 m of sliding, the incremental wear of the sample is decreasing. However, after this point, the incremental wear begins to increase before achieving a steady-state wear of $1.5 \times 10^{-4} \text{ mm}^3/\text{Nm}$. The volume loss and steady-state wear behavior is observed in Figure 8a. The self-mated countersample followed a similar trend but maintained a lower total and incremental wear rate than the self-mated pin and achieved a steady-state wear rate of $4.0 \times 10^{-5} \text{ mm}^3/\text{Nm}$ (Figure 8a). The increase in wear at 800 m of sliding could be caused by several factors. One possibility is similar to that of the PTFE alumina sample, where the transfer film forms but begins to delaminate and leads to a large wear event. The unfilled PTFE pin exhibited significant amounts of creep, causing the sample width to increase and the contact patch and wear track on the polymer sample to increase, which could have also contributed to increases in wear. Wear testing of the self-mated unfilled PTFE sample was stopped at 4 km of sliding due to high mass loss and lack of remaining pin length to test.

The IR spectra of the worn surfaces of the self-mated and on-steel unfilled PTFE samples, as well as the unworn bulk composite, are shown in Figure 8b. The unworn and worn on-steel surfaces are the same with no noticeable peak variation except for a slightly larger 1204 cm^{-1} peak. There was no evidence of an increase in carboxyl peaks (~ 1650 and $\sim 1450 \text{ cm}^{-1}$) from unworn to worn samples, thus no significant accumulation of tribochemical species. The spectrum of the

self-mated sample is similar to that of the worn-on steel but displays peak broadening at 1149 cm^{-1} . The broadening of this peak likely indicates degradation of PTFE in the near-surface region. There is a slight absorbance at 1254 cm^{-1} in the self-mated spectrum, which has previously been attributed to alignment of PTFE chains.^{13,44} Additionally, a small increase at 1300 cm^{-1} in the self-mated sample can also be attributed to the shortening of PTFE chains (Table 1). The overall differences in the IR spectra of the self-mated and on-steel samples indicated some change in the self-mated surface that is not typical of lower wear samples. The improved wear and friction behavior of self-mated unfilled PTFE may simply be a result of the interaction of two low surface energy materials as opposed to a steel countersample that is more likely to adhere to PTFE through interatomic forces; for example, the Hamaker constant of PTFE–PTFE is reported to be significantly lower (~ 3.63 to 6.02) than that of PTFE and metals (e.g., Ag-PTFE: 8.34 – 16.44 ; Cu-PTFE: 8.72 – 14.92).⁵⁰ The increased wear on steel could also be attributed to high contact–pressure interactions with steel asperities that could be damaging, as opposed to lower contact pressures in the self-mated case. In addition, the alignment of the PTFE chains at a molecular level is more favorable in the self-mated configuration, as indicated by the shoulder at 1254 cm^{-1} ; this could also reduce the wear of the material.

4. MECHANISTIC DISCUSSION

4.1. Self-Mated PTFE-Alumina. In this study, the self-mated PTFE-alumina composites exhibited exceptional wear rates and friction coefficients. However, their wear rates and friction coefficients were higher when compared to samples slid against steel. Ultralow wear PTFE-alumina composites rely on the breakdown and accumulation of alumina at the sliding interface to create robust transfer films.¹² A countersurface such as stainless steel has a high-enough hardness to break down friable alumina particles during sliding. However, when sliding in self-mated configuration, a low wt % PTFE-alumina composite is mostly sliding against PTFE. In an alumina-on-PTFE contact, the hardness of the alumina particles makes it difficult to imagine a scenario in which PTFE can break them. It is possible that two alumina particles contact each other and break; however, the frequency of this occurrence is expected to be much less. Additionally, although the IR spectra show the existence of perfluorinated carboxylates in the worn self-mated-configuration, a significantly lower absorbance near 800 cm^{-1} (metal-oxo species from alumina) points to the lack of alumina particle breakdown and accumulation in the running film.

One function of alumina accumulation in the PTFE-alumina tribofilms is reinforcement of the polymer surface and near-surface regions. This surface layer has been observed to have more than 50% alumina by volume, as composed to the bulk composite of $\sim 2.8\%$ alumina by volume.¹² This results in it being significantly harder.¹⁶ Creep is a significant factor in PTFE with the applied loads used for testing, as the contact pressure used in testing approaches half of the reported yield strength of PTFE.⁵¹ Polymer pins for wear experiments are initially machined to square $\sim 6.35 \times 6.35\text{ mm}$ cross sections. With most experiments that we run on PTFE-based systems, we do not see this dimension change significantly. However, the area of the sliding surface of the self-mated PTFE-alumina pin increased by 10%, from ~ 40 to $\sim 44\text{ mm}^2$, a result of plastic deformation, presumably from creep. The PTFE-alumina slid on steel did not deform, which indicated that the tribofilm was

mechanically robust due to the increased alumina composition; this alumina accumulation limits creep, a major failure mode of PTFE. In the case of unfilled PTFE on steel, we generally do not observe creep; however, creep is likely occurring, but the evidence (a widened contact surface) is likely worn before it can be observed because of the high wear rate of unfilled PTFE. Surprisingly, for the self-mated unfilled PTFE sample, the area of the sliding surface visibly increased, presumably because we were able to slide much longer due to the lower wear rate in the self-mated, whereas in typical PTFE on steel experiments, the pin is not loaded long enough to observe creep (or perhaps it is wearing too fast to observe creep).

The self-mated PTFE-alumina pin does undergo an ultralow wear transition region ($\sim 2.1 \times 10^{-8}\text{ mm}^3/\text{Nm}$ between $\sim 50\text{k}$ and 100k cycles) similar to that reported with PTFE-alumina on steel. However, it then increases by approximately an order of magnitude for the remaining 900k cycles. Similarly, the countersample in the self-mated PTFE-alumina reaches a minimum wear rate ($\sim 2.5 \times 10^{-8}\text{ mm}^3/\text{Nm}$ between $\sim 500\text{k}$ and 600k cycles). It also then increases by approximately an order of magnitude for the remaining cycles. Without intermediate IR measurements, it is hard to speculate how the tribofilms evolve during these transitions in wear rates. In the case of PTFE-alumina on steel, the accumulation of alumina filler fragments can also play a role as an anchor for the tribochemically degraded PTFE, forming bonds between the carboxyl group and the accumulated metal and metal oxides.

In the self-mated PTFE-alumina, the countersample has significantly lower surface energy than a steel countersample. The IR suggests that there is also less tribochemically degraded PTFE accumulation in the self-mated PTFE/alumina as compared to sliding on steel. Third-body wear debris is more likely to stick to steel than a PTFE/alumina countersample. This would result in third-body debris fragments being maintained in the contact longer, causing more degradation of the PTFE (carboxylate groups) and increasing the probability of it remaining stuck in the contact with each new carboxylate anchor formed. Ye et al. have recently reported that a gradient in surface energy drives the direction and magnitude of system wear.⁵² They suggest that in a PTFE-alumina on steel system, the surface energy increases as you progress from the bulk polymer, through the polymer wear surface (running film), then the transfer film, and finally to the steel countersample; this sets a general flow of tribochemically generated material from the pin to the transfer film. They find that the difference of the surface energy between the polymer wear surface and the transfer film is critical for the wear rate and stability of the transfer film. An optimal case exists when the surface energy of the running film is lower than the transfer film by just enough to create an ideal balance of tribochemical wear and subsequent incorporation of worn species into the transfer film. In other words, the wear of the polymer surface matches the replenishment needs of the transfer film with a safety factor. If the surface energy of the transfer film is too high relative to the polymer wear surface, there is higher wear of the polymer with the formation of a stable transfer film. If the direction of the gradient is flipped, the transfer film may become unstable (i.e., wear or delaminate).

In the case of self-mated PTFE, a surface energy gradient for transfer film stability is unnecessary. It seems that sliding on PTFE-alumina, even in the self-mated case, creates an inherently wear-resistant surface. The mechanisms associated

with this are likely tied to accumulation of alumina at the wear surface, bound by carboxylate groups on tribochemically reacted PTFE fragments. In this system, the alumina also serves to shut down the large-scale delamination wear mechanisms routinely achieved by filling PTFE with just about anything.^{14,15,19} The formation of tribochemistry results in higher attractive energies between the sliding surfaces. This, combined with the potentially lower level of adhesion between the film and the countersample/pin, can cause delamination of the film. This cycle repeats itself, causing multiple wear events and higher levels of wear rate over time. This is different from the PTFE/alumina on steel, which has a general flow of material from the pin to the transfer film.

4.2. Self-Mated PTFE–PEEK. In the case of PTFE–PEEK composites, the accumulation of PEEK at the sliding interface and the formation of carboxylates help to reinforce the tribofilms formed on steel countersurfaces, in a similar manner to the accumulation of alumina in PTFE–alumina. PTFE–PEEK in a self-mated configuration exhibits even lower wear rates and friction coefficients when compared to PTFE–PEEK slid against steel. The improved wear performance and lower friction coefficient of the self-mated configuration can be explained by the following mechanisms: (1) low surface energy of the PTFE–PEEK surface results in low friction coefficient. (2) High conformality of the surfaces and lack of abrasion contributes to low wear. (3) PEEK accumulates at and reinforces the sliding surface of the composite. (4) Minimal surface energy gradient prevents large-scale transfer of accumulated PEEK and tribochemical carboxylates (and removal). (5) Self-mated configuration negates needs for a transfer film. (6) Interpenetrating networks of PEEK and PTFE¹⁹ anchor surface films better than the particulate-reinforced PTFE–alumina.

In all self-mated samples, the pin appeared to run in faster than the countersample. This could be due to the competing development of tribofilms on each surface. Unlike the case of sliding on steel, the two sliding surfaces are degrading/wearing simultaneously. The pin is in constant contact, and for every sliding cycle, only 31% of the total countersample track length is in contact with the pin. The pin transfer film most likely experiences higher levels of degradation due to its entire surface constantly experiencing sliding affects. In previous works,⁵² interfacial surface energy gradients are necessary to drive the direction of wear. Material tends to transfer from low to high surface energies, and the rate of transfer is dependent on the magnitude of the gradient between the two. In the self-mated case, the pin is running in faster and developing high levels of tribochemistry, giving it higher levels of surface energy than the countersample. This drives wear from the countersample to be slightly higher than the wear of the pin.

Before sliding begins, the surface energies of the two materials are low and of the same magnitude. Over the course of sliding, the overall system is low wear due to a lack of a high surface energy differential. However, as the pin slides, a tribofilm develops at a faster rate due to experiencing longer periods of sliding forces; it becomes the lower wear component of the system. The lack of a large surface energy differential between surfaces allows tribofilm formation and run in to occur for both samples, but the small differential results in slightly different rates. In this case, shorter sliding strokes or constant contact in a thrust bearing configuration could result in a more similar behavior between the countersample and the pin.

Interestingly, the friction coefficients of self-mated samples increased with increasing steady-state wear rates of both the pin and the countersample (Figure 9). Conversely, the friction

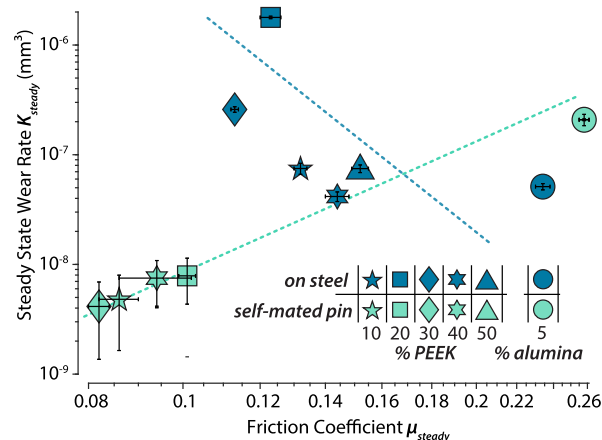


Figure 9. Steady-state wear rate plotted against friction coefficient for all the filled PTFE composites tested. The friction coefficient reported is the average friction coefficient in the steady-state wear regime of the sample. Note: Dashed lines are not trend lines but are provided to guide the eye.

coefficients decreased with increasing wear rate for the polymer composites slid against steel (Figure 9). For self-mated samples, lower friction coefficients generally correlate with lower wear rates. This is surprising for ultralow wear PTFE materials, as they have generally been reported to increase in friction with decreasing wear rates. For polymer-on-steel sliding conditions, lower wear rate is typically achieved at the expense of friction coefficient. We posit that for the case of composite-on-steel, the reduced wear rate is enabled by well-established tribofilms, which typically have a significant amount of tribochemically generated carboxyl end groups that have a greater affinity to attractively interact with the steel countersample, thus increasing the friction coefficient. Conversely, there is evidence that the wear rate scales with the amount of frictional work done when transfer film formation is not imperative. The unique finding that lower wear rates and friction coefficients can be achieved simultaneously in self-mated configurations can have immediate and significant industrial and application impacts.

5. CONCLUSIONS

Ultralow wear and low friction can be enhanced when sliding PTFE-based polymer composites in a self-mated configuration. Self-mated PTFE–PEEK achieves lower wear when compared to on-steel for all wt % compositions tested, with most achieving 10^{-9} mm³/Nm wear rates. PTFE alumina, which requires the breakdown of microscale fillers to form robust transfer films, achieves ultralow wear and forms tribochemistry but undergoes large wear events, resulting in slightly higher wear rates self-mated than when paired with steel. Surface energy gradients dominate the transport from ultralow wear PTFE composites to incorporation in transfer films on steel. Surface energy gradients are minimized in self-mated PTFE systems, negating the need to form a polymer transfer film adhered to a metallic surface. Instead, these self-mated systems rely only on the formation and stability of tribofilms that consist of tribochemically altered PTFE with new carboxylate

end groups as well as accumulated filler (i.e., PEEK or alumina). Interpenetrating networks of PEEK and PTFE are more effective at anchoring these surface films than the particulate-reinforced PTFE-alumina.

AUTHOR INFORMATION

Corresponding Author

Brandon A. Krick – Department of Mechanical Engineering, Florida Agricultural and Mechanical University, Florida State University College of Engineering, Tallahassee, Florida 32310, United States; The Aero-propulsion, Mechatronics and Energy Center, Florida State University, Tallahassee, Florida 32310, United States; orcid.org/0000-0003-3191-5433; Phone: (850) 645-0141; Email: bkrick@eng.famu.fsu.edu

Authors

Kylie E. Van Meter – Department of Mechanical Engineering, Florida Agricultural and Mechanical University, Florida State University College of Engineering, Tallahassee, Florida 32310, United States; The Aero-propulsion, Mechatronics and Energy Center, Florida State University, Tallahassee, Florida 32310, United States; orcid.org/0000-0002-1458-8664

Christopher P. Junk – Department of Materials Science and Engineering, Lehigh University, Bethlehem, Pennsylvania 18015, United States; CJIdeas, LLC, Wilmington, Delaware 19810, United States

Kasey L. Campbell – Department of Materials Science and Engineering, Lehigh University, Bethlehem, Pennsylvania 18015, United States

Tomas F. Babuska – Department of Mechanical Engineering, Florida Agricultural and Mechanical University, Florida State University College of Engineering, Tallahassee, Florida 32310, United States; The Aero-propulsion, Mechatronics and Energy Center, Florida State University, Tallahassee, Florida 32310, United States; Department of Mechanical Engineering and Mechanics, Lehigh University, Bethlehem, Pennsylvania 18015, United States

Complete contact information is available at:

<https://pubs.acs.org/10.1021/acs.macromol.1c02581>

Notes

The authors declare no competing financial interest.

ACKNOWLEDGMENTS

This material is based on the work supported by the National Science Foundation CMMI MEP #2027029 (Krick CAREER), the National Science Foundation CMMI MEP #1463141 (Krick GOALI), and the National Science Foundation Graduate Research Fellowship Program under grant #1449440 (Van Meter), #1452783 (Campbell), and #1842163 (Babuska). The authors would like to thank Cooper Atkinson and Mark Sidebottom for early efforts at making molds for large polymer plates. We would like to thank undergraduate student Brantley Balsamo for sample preparation in preliminary experiments.

REFERENCES

- (1) Renfrew, M. M.; Lewis, E. E. Polytetrafluoroethylene. Heat Resistant, Chemically Inert Plastic. *Ind. Eng. Chem.* **1946**, *38*, 870–877.
- (2) Bunn, C. W.; Howells, E. R. Structures of Molecules and Crystals of Fluoro-Carbons. *Nature* **1954**, *174*, 549–551.
- (3) Bunn, C. W.; Cobbold, A. J.; Palmer, R. P. The fine structure of polytetrafluoroethylene. *J. Polym. Sci.* **1958**, *28*, 365–376.
- (4) Shooter, K. V.; Tabor, D. The Frictional Properties of Plastics. *Proc. Phys. Soc., London, Sect. B* **1952**, *65*, 661.
- (5) Puts, G. J.; Crouse, P.; Ameduri, B. M. Polytetrafluoroethylene: Synthesis and Characterization of the Original Extreme Polymer. *Chem. Rev.* **2019**, *119*, 1763–1805.
- (6) Makinson, K. R.; Tabor, D. The friction and transfer of polytetrafluoroethylene. *Proc. R. Soc. London, Ser. A* **1964**, *281*, 49–61.
- (7) Biswas, S. K.; Vijayan, K. Friction and wear of PTFE - a review. *Wear* **1992**, *158*, 193–211.
- (8) Tanaka, K.; Uchiyama, Y.; Toyooka, S. The mechanism of wear of polytetrafluoroethylene. *Wear* **1973**, *23*, 153–172.
- (9) Deli, G.; Qunji, X.; Hongli, W. Study of the wear of filled polytetrafluoroethylene. *Wear* **1989**, *134*, 283–295.
- (10) Blanchet, T. A.; Kennedy, F. E. Sliding wear mechanism of polytetrafluoroethylene (PTFE) and PTFE composites. *Wear* **1992**, *153*, 229–243.
- (11) Sawyer, W. G.; Freudenberg, K. D.; Bhimaraj, P.; Schadler, L. S. A study on the friction and wear behavior of PTFE filled with alumina nanoparticles. *Wear* **2003**, *254*, 573–580.
- (12) Krick, B. A.; et al. Ultralow wear fluoropolymer composites: Nanoscale functionality from microscale fillers. *Tribol. Int.* **2016**, *95*, 245–255.
- (13) Harris, K. L.; et al. PTFE Tribology and the Role of Mechanochemistry in the Development of Protective Surface Films. *Macromolecules* **2015**, *48*, 3739–3745.
- (14) Burris, D. L.; et al. A route to wear resistant PTFE via trace loadings of functionalized nanofillers. *Wear* **2009**, *267*, 653–660.
- (15) Alam, K. I.; Baratz, A.; Burris, D. Leveraging trace nanofillers to engineer ultra-low wear polymer surfaces. *Wear* **2021**, *483*, 203965.
- (16) Krick, B. A.; Ewin, J. J.; McCumiskey, E. J. Tribofilm Formation and Run-In Behavior in Ultra-Low-Wearing Polytetrafluoroethylene (PTFE) and Alumina Nanocomposites. *Tribol. Trans.* **2014**, *57*, 1058–1065.
- (17) Burris, D. L.; Sawyer, W. G. Tribological Sensitivity of PTFE/Alumina Nanocomposites to a Range of Traditional Surface Finishes. *Tribol. Trans.* **2005**, *48*, 147–153.
- (18) Pitenis, A. A.; et al. Ultralow Wear PTFE and Alumina Composites: It is All About Tribochemistry. *Tribol. Lett.* **2015**, *57*, 4.
- (19) Burris, D. L.; Sawyer, W. G. A low friction and ultra low wear rate PEEK/PTFE composite. *Wear* **2006**, *261*, 410–418.
- (20) Haidar, D. R.; Alam, K. I.; Burris, D. L. Tribological Insensitivity of an Ultralow-Wear Poly(etheretherketone)-Polytetrafluoroethylene Polymer Blend to Changes in Environmental Moisture. *J. Phys. Chem. C* **2018**, *122*, 5518–5524.
- (21) Campbell, K. L.; et al. Ultralow Wear PTFE-Based Polymer Composites-The Role of Water and Tribochemistry. *Macromolecules* **2019**, *52*, 5268–5277.
- (22) Krick, B. A.; et al. Environmental dependence of ultra-low wear behavior of polytetrafluoroethylene (PTFE) and alumina composites suggests tribochemical mechanisms. *Tribol. Int.* **2012**, *51*, 42–46.
- (23) Tanaka, K. Effects of Various Fillers on the Friction and Wear of PTFE-Based Composites. *Compos. Mater. Ser.* **1986**, *1*, 137–174.
- (24) Sawyer, W. G.; Argibay, N.; Burris, D. L.; Krick, B. A. Mechanistic Studies in Friction and Wear of Bulk Materials. *Annu. Rev. Mater. Res.* **2014**, *44*, 395–427.
- (25) Ye, J.; Khare, H. S.; Burris, D. L. Transfer film evolution and its role in promoting ultra-low wear of a PTFE nanocomposite. *Wear* **2013**, *297*, 1095–1102.
- (26) Burris, D. L.; Boesl, B.; Bourne, G. R.; Sawyer, W. G. Polymeric Nanocomposites for Tribological Applications. *Macromol. Mater. Eng.* **2007**, *292*, 387–402.
- (27) Ye, J.; Haidar, D.; Burris, D. L. Transfer film properties and their role in polymer wear In *Handb. Polym. Tribol.*; World Scientific Publishing Co. Pte. Ltd., 2018, pp 269–303

- (28) Ye, J.; Haidar, D.; Burris, D. Polymeric Solid Lubricant Transfer Films: Relating Quality to Wear Performance. *Self-Lubricating Compos.* **2018**, 155–180.
- (29) Uruëa, J. M.; Pitenis, A. A.; Harris, K. L.; Sawyer, W. G. Evolution and wear of fluoropolymer transfer films. *Tribol. Lett.* **2015**, 57, 9.
- (30) Biswas, S. K.; Vijayan, K. Friction and wear of PTFE - a review. *Wear* **1992**, 158, 193–211.
- (31) Pitenis, A. A.; Ewin, J. J.; Harris, K. L.; Sawyer, W. G.; Krick, B. A. In Vacuo Tribological Behavior of Polytetrafluoroethylene (PTFE) and Alumina Nanocomposites: The Importance of Water for Ultralow Wear. *Tribol. Lett.* **2013**, 53, 189–197.
- (32) Sidebottom, M. A.; et al. Perfluoroalkoxy (PFA)- α -Alumina Composites: Effect of Environment on Tribological Performance. *Tribol. Lett.* **2020**, 68, 14.
- (33) Khare, H. S.; et al. Interrelated Effects of Temperature and Environment on Wear and Tribochemistry of an Ultralow Wear PTFE Composite. *J. Phys. Chem. C* **2015**, 119, 16518–16527.
- (34) Onodera, T.; Park, M.; Souma, K.; Ozawa, N.; Kubo, M. Transfer-Film Formation Mechanism of Polytetrafluoroethylene: A Computational Chemistry Approach. *J. Phys. Chem. C* **2013**, 117, 10464–10472.
- (35) Onodera, T.; et al. Effect of Tribochemical Reaction on Transfer-Film Formation by Poly(tetrafluoroethylene). *J. Phys. Chem. C* **2014**, 118, 11820–11826.
- (36) MAKINSON, K. R.; TABOR, D. Friction and Transfer of Polytetrafluoroethylene. *Nat* **1964**, 201, 464–466 1964 2014918 201.
- (37) Krick, B. A.; Hahn, D. W.; Sawyer, W. G. Plasmonic diagnostics for tribology: In situ observations using surface plasmon resonance in combination with surface-enhanced raman spectroscopy. *Tribol. Lett.* **2013**, 49, 95–102.
- (38) Schmitz, T. L.; Action, J. E.; Burris, D. L.; Ziegert, J. C.; Sawyer, W. G. Wear-rate uncertainty analysis. *J. Tribol.* **2004**, 126, 802–808.
- (39) Burris, D. L.; Sawyer, W. G. Addressing Practical Challenges of Low Friction Coefficient Measurements. *Tribol. Lett.* **2009**, 35, 17–23.
- (40) Przedlacki, M.; Kajdas, C. Tribochemistry of Fluorinated Fluids Hydroxyl Groups on Steel and Aluminum Surfaces. *Tribol. Trans.* **2006**, 49, 202–214.
- (41) Kajdas, C. K. Importance of the triboemission process for tribochemical reaction. *Tribol. Int.* **2005**, 38, 337–353.
- (42) Al Lafi, A. G. FTIR spectroscopic analysis of ion irradiated poly(ether ether ketone). *Polym. Degrad. Stab.* **2014**, 105, 122–133.
- (43) Vanni, H.; Rabolt, J. F. Fourier transform infrared investigation of the effects of irradiation on the 19 and 30°C phase transitions in polytetrafluoroethylene. *J. Polym. Sci., Polym. Phys. Ed.* **1980**, 18, 587–596.
- (44) Lauer, J. L.; Bunting, B. G.; Jones, W. R. J., Jr. Investigation of Frictional Transfer Films of PTFE by Infrared Emission Spectroscopy and Phase-Locked Ellipsometry. *Tribol. Trans.* **1988**, 31, 282–288.
- (45) Moynihan, R. E. The Molecular Structure of Perfluorocarbon Polymers. Infrared Studies on Polytetrafluoroethylene I. *J. Am. Chem. Soc.* **2002**, 81, 1045–1050.
- (46) Liang, C. Y.; Krimm, S. Infrared Spectra of High Polymers. III. Polytetrafluoroethylene and Polychlorotrifluoroethylene. *J. Chem. Phys.* **2004**, 25, 563.
- (47) Burris, D. L.; Sawyer, W. G. Tribological behavior of PEEK components with compositionally graded PEEK/PTFE surfaces. *Wear* **2007**, 262, 220–224.
- (48) Lenk, T. J.; et al. Structural Investigation of Molecular Organization in Self-Assembled Monolayers of a Semifluorinated Amidethiol. *Langmuir* **2002**, 10, 4610–4617.
- (49) Burris, D. L.; Sawyer, W. G. Improved wear resistance in alumina-PTFE nanocomposites with irregular shaped nanoparticles. *Wear* **2006**, 260, 915–918.
- (50) Eichenlaub, S.; Chan, C.; Beaudoin, S. P. Hamaker Constants in Integrated Circuit Metalization. *J. Colloid Interface Sci.* **2002**, 248, 389–397.
- (51) Nunes, L. C. S.; Dias, F. W. R.; Da Costa Mattos, H. S. Mechanical behavior of polytetrafluoroethylene in tensile loading under different strain rates. *Polym. Test.* **2011**, 30, 791–796.
- (52) Ye, J.; et al. Interfacial Gradient and Its Role in Ultralow Wear Sliding. *J. Phys. Chem. C* **2020**, 124, 6188–6196.

Recommended by ACS

Surface Fatigue Behavior of a WC/aC:H Thin-Film and the Tribochemical Impact of Zinc Dialkyldithiophosphate

Siavash Soltanahmadi, Anne Neville, et al.

OCTOBER 14, 2019
ACS APPLIED MATERIALS & INTERFACES

READ 

Enhancement of Underwater Tribological Properties of Hybrid PTFE/Nomex Fabric/Epoxy Resin Multilayer Composites by Mixed Graphite and MoS₂ Fillers

Ying Liu, Zhongwei Yin, et al.

JULY 27, 2022
ACS OMEGA

READ 

Wear Resistance Mechanism of Ultrahigh-Molecular-Weight Polyethylene Determined from Its Structure–Property Relationships

Huan Zhang, Jincheng Xia, et al.

SEPTEMBER 26, 2019
INDUSTRIAL & ENGINEERING CHEMISTRY RESEARCH

READ 

Moderate Chain Branching in Waterborne Pressure-Sensitive Adhesives Combines Strain Hardening with Entanglements Formed during Film Formation: A S...

Christopher Hirth, Diethelm Johannsmann, et al.

JULY 14, 2022
MACROMOLECULES

READ 

Get More Suggestions >